BAR-ILAN UNIVERSITY

Spintronics in Itinerant $3d$ and $4d$ Ferromagnets

ISASCHAR GENISH

Department of Physics

Ph.D. Thesis

Submitted to the Senate of Bar-Ilan University

Ramat-Gan, Israel April 2009

This work was carried out under the supervision of

Professor Lior Klein

Department of Physics

Bar-Ilan University

Acknowledgments

The years of my study were a wonderful educational period that gave me the opportunity to be involved in scientific research. Many researchers, some of whom became my friends, enabled me to add my humble contribution to several works in the fields of physics and chemistry. To the good people that taught me and worked with me I would like to express my thanks.

First, I would like to thank my advisor, Prof. Lior Klein, who introduced me into experimental solid state physics, gave me an opportunity to be involved in every aspect of a research work, and allowed me to test some of my ideas freely. I much appreciate his great dedication to his students and his advice.

I also want to thank Yevgeny Kats, an amazing person who at some stage of his research, worked on his Ms.c. thesis in parallel with me, and contributed much to the work presented here. I would also wish to thank Yishay Shperber with whom I have done some research concerning permalloy and $SrRuO_3$.

I thank my dear friends Moty Schultz and Yosi Bason who collaborated with me in building a room temperature measuring device.

I want to thank several members from the chemistry department at Bar-Ilan university: From Prof. Doron Aurbach's laboratory I would like to thank Dr. Gregory Salitra, a very skilled physicist who fabricated our permalloy films that were necessary for the work concerning permalloy sensors, and together with Dr. Elad Pulak allowed me to participate in an interesting work on Carbon Molecular Sieve Electrodes. I thank Dr. Yosef Talyosef for making me part of his work on lithium ion cells. From Prof. Aharon Gedanken's laboratory I would like to give a special thanks to Prof.

Gedanken himself for his kind advice and his part in one of my research projects. I would also like to thank Dr. David S. Jacob, a very diligent man, who allowed me to take part in his work on Core Shell Copper and Nickel Nanoparticles. I would like to express my thanks to Dr. Ramakrishnan Kalai, a post doctoral student from India, that gave me the opportunity to take part in his work on Synthesis of Submicron-Sized Rare Earth Hexaborides.

I also wish to thank Alex Irzh from Prof. Aharon Gedanken's laboratory and Assaf Anderson from Prof. Arie Zaban's laboratory both from the chemistry department at Bar - Ilan university, for their share in the new discovery about plasma layer coating; a patent is pending, and for their part in an article submitted concerning plasma reduction of metallic ions. I thank Alex Irzh also for the opportunity to be part on a work concerning air-stable zinc nanoparticles.

I had the honor to work with some people from abroad that assisted me in my work or gave me the opportunity to be part of theirs:

I wish to thank Prof. Marcin Konczykowski from the "Laboratoire des Solides Irradies" for his hospitality when I worked together with him on irradiation of $SrRuO_3$ samples at the École Polytechnique, Palaiseau, France.

I would like to thank Dr. Jim Reiner, a former member of the KGB group at Stanford University, who made his excellent samples of $SrRuO_3$ available to us.

I thank Dr. Raisa Apostolova from the Ukraine that enabled me to be involved in her work on lithium batteries.

I also thank the secretaries of the department of physics, Rachel Rotberg and Sara Bialkovitch, that always found time help me in any way they could. I thank Dr.

Orit Chasid and Dr. Efrat Bodner who made all the bureaucratical arrangements concerning my work as the High-Resolution Scanning Electron microscope operator.

It has been a great pleasure for me to share the lab with Yevgeny Kats, Shahar Levy, Dr. Michael Feigenson, Moty Schultz, Yosi Bason, Nati Naftalis, Yishai sh-perber, Snir Seri and the three new members Alex Kaplan, Vlad Murashenko and Yevgeny Telepinsky.

Finally, I want to thank my family: My parents, my brother and my sisters for their support. Last but not least I would like to thank my wonderful wife Shani, my source of joy, who helped me and supported me over the years.

List of Publications

Paramagnetic anisotropic magnetoresistance in thin films of $SrRuO_3$

Isaschar Genish, Yevgeny Kats, Lior Klein, James W. Reiner, and M. R. Beasley;

J. appl. Phys., 95, 6681 (2004).

Testing the Berry phase model for extraordinary Hall effect in $SrRuO_3$

Yevgeny Kats, Isaschar Genish, Lior Klein, James W. Reiner, and M. R. Beasley;

Phys. Rev. B., 70, 180407(R), (2004).

Local measurements of magnetization reversal in thin films of $SrRuO_3$

Isaschar Genish, Yevgeny. Kats, Lior Klein, James W. Reiner, and M. R. Beasley;

Phys. stat. sol. (C), 1 3440, (2004).

Large anisotropy in the paramagnetic susceptibility of $SrRuO_3$ films

Yevgeny Kats, Isaschar Genish, Lior Klein, James W. Reiner, and M. R. Beasley;

Phys. Rev. B., 71, 100403(R), (2005).

The Dependence of the Electronic Conductivity of Carbon Molecular Sieve Electrodes on Their Charging States

Elad Pollak, Isaschar Genish, Gregory Salitra, Abraham Soffer, Lior Klein, and Doron Aurbach;

J. phys. Chem. B., 110, 7443, (2006).

Carbon-Coated Core Shell Structured Copper and Nickel Nanoparticles Synthesized in an Ionic Liquid

David S. Jacob, Isaschar Genish, Lior Klein, and Aharon Gedanken;

Phys. Chem. Lett., 110, 17711, (2006).

Determination of the resistivity anisotropy of $SrRuO_3$ by measuring the planar Hall effect

Isaschar Genish, Lior Klein, James W. Reiner, and M. R. Beasley;

Phys. Rev. B., 75, 125108, (2007).

New developments of $LiNi_{0.5}Mn_{O.5}O_2$ electrodes comprising micro - and nano - metric particles: Synthesis, electrochemical behavior, and surface chemistry in Li-ion cells

Yosef Talyosef, Daniela Kovacheva, Ronit Levi, Mila Gorova, Judith Grinblat, Isaschar Genish, Boris Markovsky, Doron Aurbach;

25^{th} International Power Sources Symposium & Exhibition, IPSS, (2007).

Electrolytic nanosized cobalt sulfides for lithium batteries

R. Apostolova, E. Shembel, Y. Talyosef, A. Mitelman, J. Grinblat, I. Genish, B. Markovsky, D. Aurbach;

8th Advanced Batteries and Accumulators - ABA-2007, 23, (2007).

Single Step, Low-Temperature Synthesis of Submicron-Sized Rare Earth Hexaborides

Ramakrishnan Kalai Selvan, Isaschar Genish, Ilana Perelshtein, Jose M. Calderon Moreno, and Aharon Gedanken;

J. Phys. Chem. C., 112, 1795, (2008).

Field induced resistivity anisotropy in $SrRuO_3$ films

Yishai Sheperber, Isaschar Genish, James W. Reiner, Lior Klein;

J. Appl. Phys., 105, 07B106-1 (2009).

Plannar Hall effect sensors - effects of shape and size

Isaschar Genish, Yishai Sheperber, Gregory Saltira, Doron Aurbach , Lior Klein;

submitted.

Coating dielectric substrates by plasma-reduction of metallic ions in solvents[1]

Isaschar Genish, Alexander Irzh, Aharon Gedanken, Assaf Anderson, Arie Zaban, and Lior Klein;

submitted.

[1]Pended to patent

Deposition of air-stable zinc nanoparticles on glass slides by the Solvent-Assisted Deposition in Plasma (SADIP) method

Irzh Alexander, Isaschar Genish, Ling Yong Chien, Chen Bo-Jung, Klein Lior, Gedanken Aharon;

submited.

Contents

Abstract

Although the influence of magnetization on the transport properties has been investigated for more than a century, this field has attracted in recent years considerable interest with the emerging of the field of spintronics ("spin transport electronics") which addresses the role of the electron spin in transport properties of magnetic metals and heterostructures consisting of magnetic metals. The importance of this field was recently recognized by the Nobel prize committee which awarded Albert Fert and Peter Grünberg the Nobel prize in the field of physics (in 2007) for their discovery of the giant magnetoresistance effect (GMR).

In this work I present results concerning the interplay between magnetization ($\mathbf{M}$) and electrical transport in the $4d$ itinerant ferromagnet $SrRuO_3$ and in nickel iron alloys (permalloy Py).

The first part concerns the pseudocubic perovskite $SrRuO_3$ which has attracted considerable interest due to its unusual transport and magnetic properties. These properties include: large resistivity that grows with temperature almost without saturation and seems to cross the Ioffe-Regel limit; deviation of the derivative of the resistivity from the Fisher-Langer theory; deviation from Matthison's rule and deviation of terahertz and infrared conductivity from Fermi liquid behavior.

The paper "*Determination of the resistivity anisotropy of $SrRuO_3$ by measuring*

the planar Hall effect" provides a comprehensive description of the spontaneous resistivity anisotropy of $SrRuO_3$ below and above the Curie temperature by measuring the planar Hall effect, which provides information on local resistivity anisotropy on patterns with current paths oriented in different crystallographic directions. We determined both magnetic and non-magnetic sources of anisotropy present in epitaxial films of $SrRuO_3$ and found that non-magnetic anisotropy makes the resistivity along $[1\bar{1}0]$ larger while spontaneous magnetization (along [010]) decreases this anisotropy. As far as we know this is the first time that such a method was applied in order to determine resistivity anisotropy, and it can also be applied in other cases in which the resistivity anisotropy is too small to be determined by other methods.

The paper "*Paramagnetic anisotropic magnetoresistance in thin films of $SrRuO_3$*" discusses the way the electrical resistivity is influenced above the Curie temperature by magnetization induced along different directions. In this article we show that the change in resistivity is affected by the angles of the current and the magnetization relative to the crystal lattice. In order to determine the direction of magnetization, we measured the extraordinary Hall effect. Measuring the anisotropic magnetoresistance (AMR) of $SrRuO_3$ with simultaneous measurements of $\mathbf{M}$ and of the magnetoresistance (MR) enabled us to preform accurate determination of its AMR behavior despite the change in the magnitude of $\mathbf{M}$ and in its relative angle with the external magnetic field ($\mathbf{H}$) due to magnetocrystaline anisotropy. The results indicate significant AMR even in the paramagnetic state, where $\mathbf{M}$ is relatively small, and large effects of crystal symmetry exist.

The third paper *"Local measurements of magnetization reversal in thin films of*

$SrRuO_3$" addresses mechanisms of magnetization reversal in $SrRuO_3$ using the extraordinary Hall effect for local monitoring. We found that the magnetic nucleation and the magnetic propagation are affected by different defects in the sample. In our experiment we observed three distinct events that could be either a nucleation event followed by propagation, or a domain wall depinning followed by propagation. Either way, the importance of the paper is in demonstrating the possibility of following distinct events locally.

The second part of the work concerns permalloy. This compound is one of the most widely used magnetic materials. The fact that it has a large magnetotransport effects made it one of the leading candidates for various applications. One of these applications concerns the ability to measure magnetic fields via its resistivity anisotropy.

In the paper: "*Planar hall effect sensors - effects of shape and size*" we explore the effects of shape and size on properties of magnetic sensors based on the planar Hall effect. We present measurements of thin-film permalloy sensors in the form of ellipses having different aspect ratios along with extensive numerical simulations. We identify upper limits above which hysteresis effects intensify, and lower limits below which the remanent state is unstable, and address the role of the ratio between the sensor thickness to its other dimensions. This work may form the basis for designing more sensitive planar Hall effect magnetic sensors.

The last section of the thesis is dedicated to a novel method of fabricating layers and particles. This new development, pending a patent, uses plasma to reduce liquid solutions into metallic layers or into particles. The ability to reduce magnetic material

is especially interesting for future spintronics applications.

The paper: "*Coating dielectric substrates by plasma-reduction of metallic ions in solvents*" discusses this new process and demonstrates its ability to fabricate magnetic and non magnetic layers as well as particles with different sizes controlled by several parameters including the solution concentration.

In this thesis I have explored different aspects of spintronics: I developed new techniques for fabrication (plasma reduction), I explored basic transport and magnetotransport phenomena (AMR and PHE) and I obtained better insight on magnetization processes and the role of different defects. Finally, I implemented the new insight I have achieved by combining experimental work, numerical simulations and theoretical models to explore different regimes of behavior of magnetic sensors. I hope that the new results of this thesis will serve as basis for further basic and applicative research.

Chapter 1

Background

1.1 Magnetic Anisotropy

Magnetic Materials exhibit a wide range of anisotropies: magnetocrystalline anisotropy, shape anisotropy, stress anisotropy, induced anisotropy (by magnetic annealing, plastic deformation or by irradiation), exchange anisotropy, and more. In this work, I consider magneto-crystalline and shape anisotropy.

1.1.1 Magnetocrystalline Anisotropy

Measurements of crystalline magnetic samples occasionally show that different fields are required to orient the magnetization in different directions - this behavior is a result of magnetocrystaline anisotropy. The direction at which a crystalline sample can be saturated with the lowest field is called the easy axis (EA) of magnetization, while the direction that needs the highest field in order to exhibit saturation is called the hard axis (HA). Figure 1.1 shows a manifestation of magnetocrystaline anisotropy (MCA) in crystalline iron [1, 2]. We see that it is easier to magnetize this crystal when an external magnetic field is oriented along its [100] direction rather then if it is oriented along either the [110] or the [111] directions.

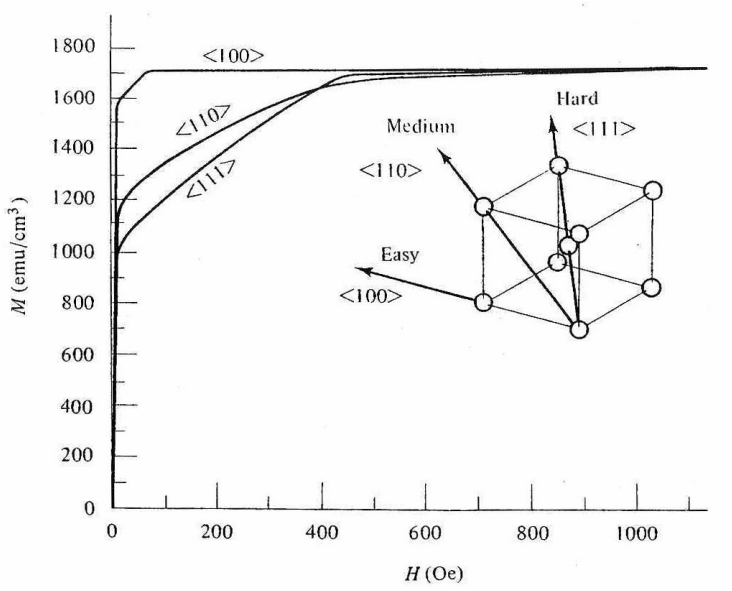

Figure 1.1: Magnetization curves for single crystal of iron [3].

Since an external magnetic field must do work against the anisotropy force in order to turn the magnetization away from the EA direction, there must be an energy stored in the crystal in the case where the saturated magnetization points at a non-EA direction. This energy is called the *crystal anisotropy energy* and can be expressed in terms of series expansions of the direction cosine of the saturated magnetization relative to the crystal axes (this treatment was done by the Russian scientist Akulov in 1929 [4] and was dealt extensively by others [5, 6, 7]). For a cubic crystal the crystal anisotropy energy is:

$$E = K_0 + K_1(\alpha_1^2\alpha_2^2 + \alpha_2^2\alpha_3^2 + \alpha_3^2\alpha_1^2) + K_2(\alpha_1^2\alpha_2^2\alpha_3^2) + ... \tag{1.1}$$

where K_0;K_1;K_2... are the anisotropy constants and α_1, α_2 and α_3 are the cosines of the angles between the magnetization and the crystal axis.

The first part of our work deals with films of $SrRuO_3$. These films possess large

uniaxial MCA (estimated anisotropy field of ∼10 T) oriented at 45° out of the films plane. For the case of a uniaxial anisotropy the expression for the energy is:

$$E = K_u sin^2\theta \tag{1.2}$$

Where K_u is the the anisotropy constant and θ is the angle between the magnetization and the axis direction.

1.1.2 Shape Anisotropy

Magnetic anisotropy which depends on the sample's geometrical factors is called *shape anisotropy*. In a sample without MCA (e.g. amorphus magnetic alloys), shape anisotropy determines the preferred direction of magnetization.

The source of shape anisotropy is the demagnetization field which acts in opposite to the samples magnetization. In this case the magnetic induction field is:

$$\mathbf{B} = -\mathbf{H_d} + 4\pi\mathbf{M} \tag{1.3}$$

where $\mathbf{H_d}$ is the demagnetization field (the value of $\mathbf{H_d}$ never exceeds $4\pi M$).

The demagnetization field is proportional to the magnetization that created it with a proportional factor N_d that depends on the samples shape and can be calculated analytically for an ellipsoid.

$$\mathbf{H_d} = N_d\mathbf{M} \tag{1.4}$$

For a prolate ellipsoid (see Figure 1.3) with the major axis at the c axis, the demagnetization factors are known to be: $N_a = N_b = \frac{4\pi - Nc}{2}$, and $N_c = \frac{4\pi}{r^2-1}[\frac{r}{\sqrt{r^2-1}} ln(r +$

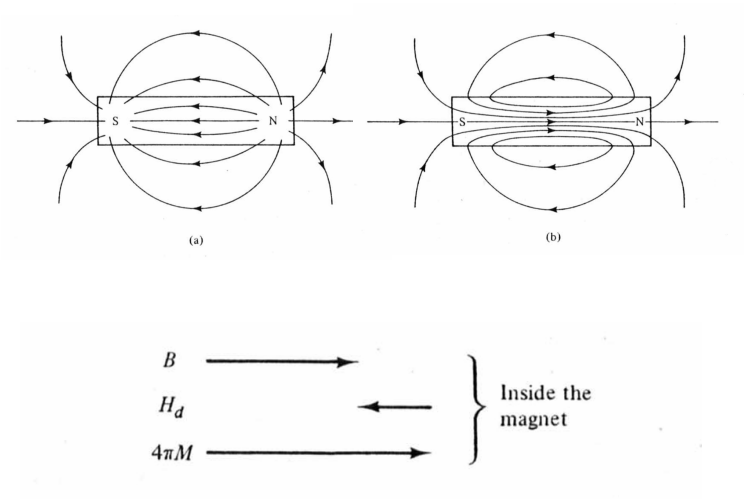

Figure 1.2: Fields of a bar magnet in Zero applied field after magnetizing it with an external field: (a) **H** field, and (b) **B** field. The vectors in the center indicate the values of these quantities at the center of the magnet [8].

$r^2 - 1$).

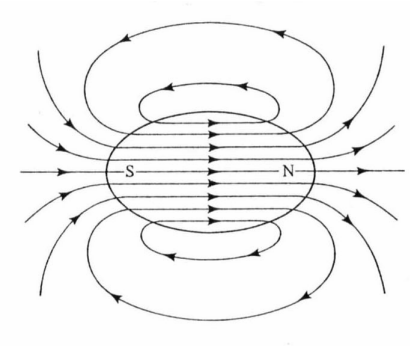

Figure 1.3: The **B** field of an ellipsoid magnet in zero applied field [9].

In general, the demagnetizing field along a short axis is stronger than that along a long axis; therefore, it is necessary to apply a higher magnetic field along the short axis in order to orient the magnetization in this direction. The associated magnetostatic energy, meaning the self-energy, or the energy of a magnet in its own field [10] is:

$$E_{ms} = \frac{1}{2} N_d M^2 \tag{1.5}$$

For prolate ellipsoid the expression of this energy is:

$$E_{ms} = \frac{1}{2} M^2 N_c + \frac{1}{2}(N_a - N_c) M^2 sin\theta \tag{1.6}$$

In this case the first term represents the role of the EA and the second term is the angle dependent part. This part can be described using the definition of the *shape-anisotropy constant*, K_s:

$$K_s = \frac{1}{2}(N_a - N_c) M^2 \tag{1.7}$$

The role of shape anisotropy is of great importance in the second part of our work where we explore polycrystalline films of Permalloy.

1.2 Magnetization Processes

By applying an external magnetic field on a magnetic sample, changes in magnetization intensity and orientation take place. Several mechanisms are responsible for these changes. Here I will discuss nucleation and single domain rotation.

1.2.1 Nucleation

When an external magnetic field is applied on a sample with an antiparallel magnetization direction, it is energetically favorable for the magnetization to flip its orientation. Since there is usually an energy barrier for this flipping, it occurs by nucleating a small region with reversal magnetization. The act of nucleation is followed by expansion propagation or of more nucleations in other areas until full reversal is achieved. The size of the nucleation area is determined by factors such as the energy gained by the magnetostatic energy and the energy loss due to exchange interaction, that is proportional to the nucleation area.

The problem of magnetic nucleation in the case of magnetization reversal was addressed by Gunther and Chudnovsky [11, 12]. They considered two states of energy minimums: local minima for the case were the magnetization is oriented to the z direction and absolute minima for magnetization pointing to the negative z direction.

The appearance of nucleation is followed by propagation until all sample space is magnetized into one single direction. We address these processes in our manuscript, *"Local measurements of magnetization reversal in thin films of $SrRuO_3$"*.

1.2.2 Single Domain Rotation

When the magnetization process occurs in a single domain particle, meaning a particle with only one magnetic domain [13, 14], applying an external magnetic field **H** at an angle α with respect to the EA, will tilt the magnetization to an angle θ with respect to the EA determined by minimization of the Stoner Wohlfarth Hamiltonian [15, 16]:

$$\mathcal{H} = K_u sin^2\theta + M_s H cos(\alpha - \theta) \tag{1.8}$$

where the first term on the right side is the contribution of the uniaxial anisotropy (crystalline or shape) and the second is due to interactions between the external field (**H**) and the saturated magnetization ($\mathbf{M_s}$). From this Hamiltonian we can find the

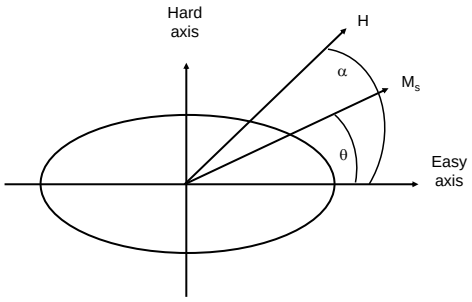

Figure 1.4: An illustration of a single magnetic domain with an ellipse shape under an external magnetic field (H)applied at an angle α with respect to the easy axis. The magnetization in this case is rotated by an angle θ from the easy axis.

equilibrium position of the magnetization by finding the extremal points.

$$\frac{d\mathcal{H}}{d\theta} = 2K_u sin\theta cos\theta - M_s H sin(\alpha - \theta) = 0 \tag{1.9}$$

or

$$sin\theta cos\theta = \frac{H}{H_K} sin(\alpha - \theta) \tag{1.10}$$

where $H_K = 2K_u/M_s$.

In our manuscript "*Planar hall effect sensors - effects of shape and size*" we present experimental results of sensors that follow the Stoner Wohlfarth Hamiltonian. In the manuscript we present also results obtained by theory and by numerical simulations that fit the experimental results.

1.3 Itinerant Magnetism

In general we distinguish between localized and itinerant magnetism. In the first case the magnetic moments are strongly connected to the atom, while in the second case the magnetic moments belong to the conduction electrons. A prominent example of an itinerant-electron system is a metallic $3d$ transition element [17]. When the $3d$ band is partially empty (Hund's rules [18]), and there exists an exchange energy (U_{eff}) due to Coulomb energy that gains energy by switching spins from being antiparallel to parallel, the interaction Hamiltonian can be written as:

$$H = U_{eff} n_1 n_2 \tag{1.11}$$

where n_1 and n_2 represent the number of electrons per atom at each spin state. Since U_{eff} is positive, the system prefers a case in which the product $n_1 n_2$ is as small as possible.

The gain in magnetic energy (ΔE_M), arising from a situation were the amount of spin up electron is the same as the number of spin down electron, to a situation where the number of one spin state is different from the other, is accompanied by an energy loss (ΔE_C) due to a change in the accommodation of electrons. Since these electrons needs to fill states of higher kinetic energy, the total change in energy must decrease. Taking into account both the gain in magnetic energy and the loss from kinetic energy and defining $N(E)$ as the density of states per spin subband we can write (for small change in the kinetic energy):

$$\Delta E = \Delta E_C + \Delta E_M = \frac{n^2 p^2}{N(E_F)}[1 - u_{eff} N(E_F)] \tag{1.12}$$

Where $p = \frac{n_1 - n_2}{2(n_1+n_2)}$ and $n = n_1+n_2$. For the non-magnetic case $p = 0$ so $-u_{eff}N(E_F) > 0$. For the ferromagnetic case $-u_{eff}N(E_{F)} < 0$ (meaning $p > 0$). The last case is known as the Stoner criterion for ferromagnetism which is used in the more familiar form:

$$U_{eff}N(E_F) > 1 \tag{1.13}$$

This condition favors a strong electron-electron interaction (Coulomb interaction) and large density of states. This criterion is roughly satisfied in the case of Fe, Co and Ni. The density of states of s and p-electrons bands is considerably smaller than that of the d band, which explains why band magnetism is restricted to elements that have a partially empty d band.

Figure 1.5 shows two band diagrams of strong and week ferromagnetism (Friedel 1969) [19].

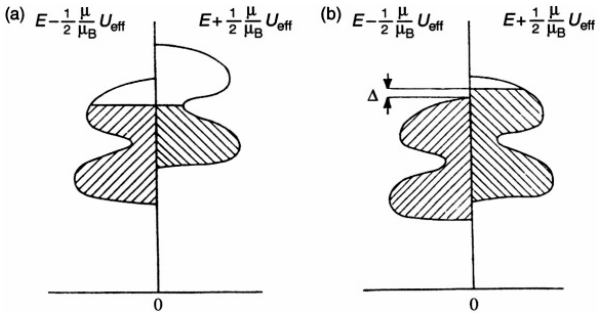

Figure 1.5: Relative position of the two half d-bands with opposite spin directions: a) week ferromagnetism. b) strong ferromagnetism. After Friedel (1969) [19].

1.4 Magnetoresistance Effects

Magnetoresistance (MR) is the relative change of the electric resistivity ρ as a result of applying a magnetic field $\mathbf{B}$,

$$MR = \frac{\rho(B) - \rho(0)}{\rho(0)} \Delta\rho/\rho(0) \tag{1.14}$$

There are several contributions to MR:

(a) *Lorentz MR.* This contribution to the MR is due to the deflection of the charge carriers from their original trajectories as a result of the Lorentz force. This effect increases the resistivity, thus creating a positive MR. The longer the mean free path (lower resistivity) relative to cyclotron radius, the larger the effect of the field on the resistance. Lorentz MR normally follows Kohler's rule [20, 21, 22]:

$$\Delta\rho/\rho(H = 0) = f(\frac{H}{\rho}) \tag{1.15}$$

(b)*Supersession of spin fluctuations.* By raising the temperature of a ferromagnetic sample, magnetic moments that tend to align, fluctuate, leading to an increase in scattering process that give rise to an increase in resistivity. By applying an external magnetic field, the fluctuating moments align in the direction of the magnetic filed, a process that reduces the scattering and the resistivity thus yielding negative magnetoresistance.

1.4.1 AMR

In 1857 William Thompson discovered that the resistivity of iron increased by 0.2% when he applied a magnetic field along the current direction, and by $\sim$0.35% when he

applied the field in a transverse direction [23, 24]. This behavior is called anisotropic magnetoresistance (AMR) [25, 26]. AMR was studied extensively [27, 28, 29, 30] for more than a century and it was used in various commercial devices including data recording devices and magnetic sensors.

The fact that the resistivity depends on the orientation of the measurement relative to the current, means that one must consider the use of the resistivity tensor. The longitudinal term describing the AMR is:

$$\rho_{long} = \rho_{\perp} + (\rho_{\parallel} - \rho_{\perp})cos^2\theta \tag{1.16}$$

For crystalline materials the terms in the resistivy tensor are more complicated and were first introduced by Döring in 1938 [31]. In this case the tensor terms are written as:

$$\rho_{ij}(\alpha) = \sum_{k,l,m...=1}^{3} (a_{ij}+a_{kij}\alpha_k+a_{klij}\alpha_k\alpha_l+a_{klmij}\alpha_k\alpha_l\alpha_m+a_{klmnij}\alpha_k\alpha_l\alpha_m\alpha_n+...) \tag{1.17}$$

where the indices i, j, k represent the different axes and the α's are the expansion coefficients.

In our work "*Determination of the resistivity anisotropy of* $SrRuO_3$" we investigated the behavior of the resistivity anisotropy in $SrRuO_3$ at the ferromagnetic and paramagnetic phases. For the paramagnetic phase, in the absence of an external magnetic field, we observed a significant resistivity anisotropy revealing the strong influence of the crystal structure. As the temperature is lowered below the critical temperature, the resistivity anisotropy behavior changes significantly, presumably due to the combined effects of the crystal structure and the external field.

1.5 Hall Effect

Charge carriers flowing in a conductor that are subject to an external magnetic field are deflected due to Lorentz force and induce a transverse electric field. This is the Hall resistance [32, 33] given by:

$$\mathbf{E} = -\frac{1}{nec} H_z J_x \widehat{y}$$

The term $-1/nec$ denoted by R_0 is the Hall coefficient. Drawing the transverse resistivity vs. the field H will produce a graph with a negative slope for electrons (negative R_0), while for holes we get a positive slope (positive R_0).

In addition to the OHE, ferromagnetic materials have another antisymmetric contribution to transverse resistance called the extraordinary Hall effect (EHE) which is related to the magnetization $\mathbf{M}$.

$$\mathbf{E_{EHE}} = R_s \mu_0 \mathbf{M}_\perp \times \mathbf{J} \tag{1.18}$$

The origin of the EHE is still controversial. In 1958 Smit suggested that spin orbit interaction leads to a deviation of the spin carriers from their initial course. This effect, known as the 'skew scattering' (see figure 1.6a), [34, 35] predicts that by taking average deflections, the EHE resistivity is proportional to ρ. Another interpretation for the 'skew scattering' is the scattering from d host states. A further development by Berger is the suggestion that the charge carriers are displaced from their original path through the scattering center mechanisms known as 'side jump' (see figure 1.6b) [36]. The EHE coefficient is therefore:

$$R_s = a\rho + b\rho^2 \tag{1.19}$$

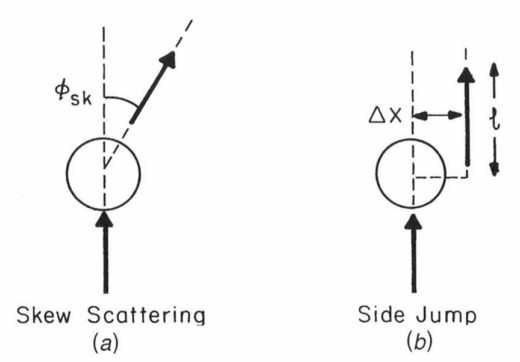

Figure 1.6: Two mechanism of EHE: (a) skew scattering and (b) side jump.

In the 1950's Karpulus and Lutinger suggested that the EHE can be explained by using the Berry phase model [37] at the k space [38, 39, 40] This model was disregarded until recently.

Since the EHE is sensitive to changes in magnetization we have used it extensively in our work. In the paper *"Paramagnetic anisotropic magnetoresistance in thin films of $SrRuO_3$"* we used the EHE as a tool for determining the magnitude and direction of magnetization in order to find its effect on the resistiviy. In the paper *"Local measurements of magnetization reversal in thin films of $SrRuO_3$"* we used this effect to determine the value at which jump in magnetization occur.

1.5.1 Planar Hall Effect

When current flows in a direction which is not one of its principle axes, it generates a transverse voltage. Although this signal is not necessarily related to magnetization, it was investigated mainly in magnetic conductors. In these cases the principle axes are determined by the direction of magnetization due to the AMR (see section 1.4.1

[25, 26]. As a consequence of AMR there is an additional contribution to the Hall signal, called the planar Hall effect (PHE) [41, 42, 43, 44].

For orthogonal principle axes the PHE signal is described using the off diagonal term of the resistivity tensor.

$$\rho_{PHE} = (\rho_{\parallel} - \rho_{\perp}) sin\theta cos\theta$$

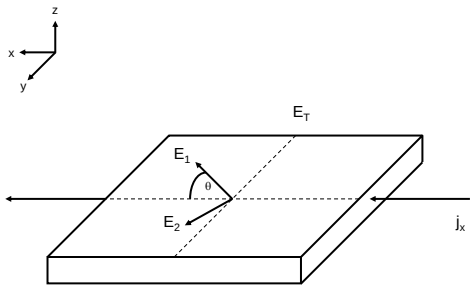

Figure 1.7: The electric fields E_1 and E_2 generated at the sample principle axes for current flowing in the x direction.

Unlike the OHE and the EHE, the PHE is symmetric with magnetization.

In our work we have used the PHE to determine the resistivity anisotropy in $SrRuO_3$ both in its paramagnetic state where it is related to the crystal structure, and below the critical temperature at its ferromagnetic state where this effect is due to the combined influences of the crystal structure and the spontaneous magnetization. The PHE is also used in our study of magnetic sensors.

1.6 Spintronics

1.6.1 General

Spintronics ("spin transport electronics"[45, 46, 47, 48, 49]), also known as magnetoelectronics, is an emerging field which exploits both the intrinsic spin of electrons in addition to their fundamental electronic charge. Although this field has its origin in the work of Mott (1936) and other works from the 1960's and the 1970's, including the works of Fert and Campbell (1968 [50], 1970 [51], 1971 [52], 1976 [53]), Tedrow and Meservey, [54] and initial experiments on magnetic tunnel junctions by Julliere [55], the most important advance in this field was achieved in the 1980's beginning with the works of Johnson and Silsbee (1985) [56], and especially due to the discovery of giant magnetoresistance simultaneously by Albert Fert et al [57], and Peter Grünberg et al [58] (1988-1989).

The use of Spintronics with other fields such as semiconductors [59] (considered theoretically already at 1990 by Datta and Das [60]) and with molecules [61, 62] are new research directions that may lead to new important results.

1.6.2 GMR and TMR

The discovery of Giant Magnetoresistance (GMR) [57, 58] is considered to be the birth of spintronics. GMR was observed in Fe/Cr/Fe multylayers where the relative alignments of the magnetic layers affected the multilayers resistance: low in parallel orientation and high in antiparallel orientation. A further development of the GMR is the GMR spin valve that consists of a trilayer structure at which the magnetization of one of the first magnetic layer is pinned to an antiferromagnetic layer, and the second

layer is magnetically free (Figure 1.8). In 1997 the GMR spin valve sensors replaced the AMR sensors in hard disk drives. As a result, the recording density increased by more then two orders of magnitude ($\sim$1 to $\sim$600 Gbit/in^2. in 2007) [49].

When the two ferromagnetic layers are separated by an insulating layer, the effect is called Tunnelling Magneto Resistance (TMR). The tunnelling resistance depends even more strongly on the relative orientation of the ferromagnetic films. It is expected that the next spintronics devices to affect the memory market would be the random access memory (MRAM) devices based on a grid of TMR cells.

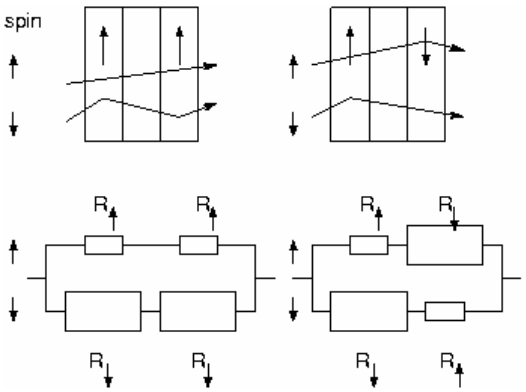

Figure 1.8: Schematic GMR structure with parallel and antiparallel alignments of the magnetic layers and an illustration of their two channel resistivities.

1.7 Magnetic Sensors

Measuring magnetic fields is of great importance in many applications. To accomplish this task, various magnetic sensors [63] have been developed including Search-Coil Sensors [64], the Flux Gate Magnetometer [65], the Optically Pumped Magnetometer [66] based on the Zeeman effect in cesium (Ce), magnetooptical sensors based on Faraday polarization effect (Fresnel ellipsoid) [67], the Fiber optic Magnetometer based on changes in interference due to path change induced by magnetostrictive materials [68, 69, 70], magnetodiode sensors based on changes in recombination due to magnetic fields [71], and magnetotransistors with two collectors giving output signal proportional to the magnetic field [72]. More examples of magnetic sensors are the nuclear precession sensor that measures the magnetic field via the proton precession frequency, the superconducting Quantum Interference (SQUID) that uses the current generated at a superconductor coil and measured via Joshepson junction [73], the OHE sensor that uses the OHE (see section 1.5), and GMR and TMR sensors (see section 1.6.2).

A very important family of magnetic sensors is based on magnetoresistive effects (see section 1.4).

In most cases, AMR sensors are based on thin films of Permalloy (Py, see section 2.2) that exhibit changeS of 3% to 4% in their resistance. MR sensors that are based on the AMR effect are widely used commercially for various applications including navigation [74] and position detectors for automotive applications [75].

A simple AMR sensor is bar shaped with its length greater than its width and a thickness that is much smaller than the other geometrical constants. A current is

then driven along its major axis and the voltage is measured along the bar.

Simple magnetoresistive sensors have several disadvantages. The first is the effect of the demagnetization field that causes a deviation in the alignment of the magnetization with respect to the current direction. The second disadvantage is the uncertainty about the sign of H_y, since R is a function of H_y^2. In addition, these AMR sensors have two other major disadvantages. The first is the fact that AMR sensors have strong non-linear dependence on the external field in the case where the transverse field is higher then the anisotropy field ($|H_y| > H_k$). Furthermore, the sensitivity dR/dH_y is very small in the proximity of the origin (and disappears entirely for $H_y = 0$). The second major disadvantage is the existence of a large noise due to temperature drift.

The problem of the demagnetization effect can be nearly resolved by changing the shape of the sensor. Some works suggest the use of an elliptical shape of the AMR array [76, 77] in order to achieve a homogeneous and small demagnetizing field.

The non linearity of the AMR sensor can be alleviated by depositing series of strips of high electrical conductivity on the magnetic layer forcing the current to flow with an angle of 45° with respect to the easy axis. This structure is called the "barber pole structure" (see Figure 1.9a, b).

In order to avoid the large noise due to temperature drift, the sensor is built as a Wheatstone bridge with four individual resistors (see Figure 1.9c). By tuning the ratio of these resistors, effects of temperature are reduced significantly. The combination of the Whetstone bridge and the barber pole structure has another advantage since a specific configuration of the barber pole angles in the different resistors, can increase the signal of these sensors.

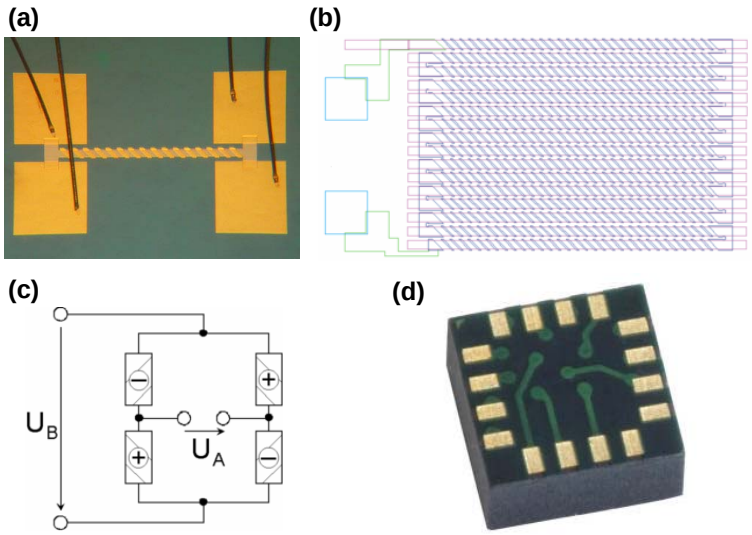

Figure 1.9: AMR sensors: a) AMR sensor with a single stripe having a layer of barber pole structure. b) array of AMR sensors. c) whetstone bridge for AMR sensors + and - signs represent barber pole with strips of 45° and 135° respectively. d) comercially 3 dimensional AMR sensor.

These improvements in the AMR sensors do not entirely eliminate the sensors' disadvantages and in some cases create new problems. The layout of the magnetoresistive elements forming a Wheatstone bridge has to be optimized and so the fabrication of these sensors become more complex. Even after optimization there is still temperature drift that reduces the device accuracy. Structure optimization concerns also the layout of width and distance of the barber poles [78] adding their contribution to the structure complexity. In addition, the well-conducting barber pole strips reduce the total resistance on the active part of the surface where changes in resistance contribute to the sensor signal.

The use of PHE (see section 1.5.1) for sensor applications enables the creation of sensors that can be the answer to these AMR disadvantages. By measuring the transverse signal (Hall configuration), the thermal drift of the output signal can be

reduced by 4 orders of magnitude [79]. PHE sensors exhibit linear response since the PHE signal changes as $\sin 2\theta$. The sensitivity of PHE sensors amplified by flux concentrators had shown a high sensitivity of 3 nT [80, 81, 82]. The linear behavior and their high sensitivity simplify their use for industrial and scientific purposes.

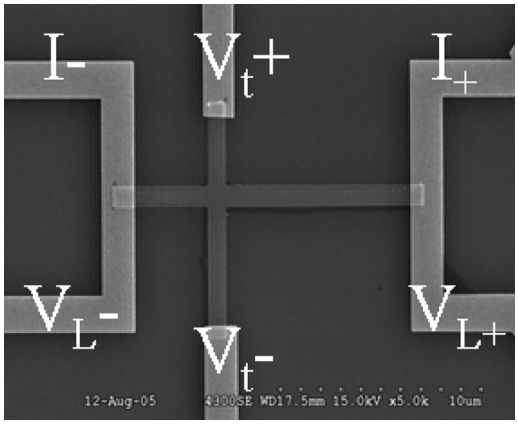

Figure 1.10: SEM image of a Permalloy cross having a width of 1 μm and a thickness of 40 nm [83].

In our work: "*Planar hall effect sensors - effects of shape and size*" we suggest the use of ellipse shape PHE sensors of Py and give new insight concerning the effect of size and shape on the sensor response. In this article we compare experimental work, numerical simulation, and theory showing the pseudo single domain behavior of these sensors. The use of numerical simulation is extended in order to determine upper and lower limits of sensor size and to determine the role of width-length ratio on the magnetic response.

Chapter 2

Materials

2.1 $SrRuO_3$

General

$SrRuO_3$ is both a metallic perovskite and a $4d$ itinerant ferromagnet. Like all perovskites [84], $SrRuO_3$ has a stoichiometric relation of $A_{n+1}B_nO_{3n+1}$ where a corner - sharing octahedra is composed of B ions at the center of each octahedron and six oxygen ions at the corners. In the center of every eight octahedra lies an A ion. In many perovskites the octahedra is tilted or rotated in order to accommodate the relatively large A ion. These distortions yield a variety of symmetries (isometric, tetragonal, nortohembral and monoclinic) depending on the degree of distortion. At room temperature, $SrRuO_3$ exhibits an orthorhombic symmetry with lattice parameters: a=5.53 Å, b=5.57 Å, and c=7.85 Å, The pseudo-cubic unit cell has a lattice parameter of 3.93 Å.

The crystalline orientation of the films of $SrRuO_3$ strongly depends on the substrate: On $SrTiO_3$ the films mostly grow with the [001] axis in the film plane [85], while some grains grow with the [001] axis perpendicular to the film plane. Much

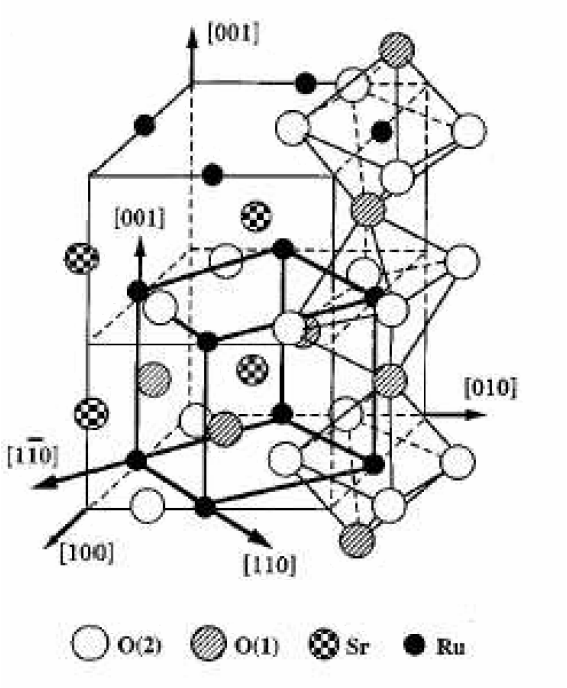

Figure 2.1: Schematic diagram of $SrRuO_3$ crystal structure in orthorhombic unit cell. The inner cube constructed by thick solid lines is the pseudo-cubic unit cell (picture from Ref. [86]).

better films of $SrRuO_3$ can be grown on miscut $SrTiO_3$ substrates. Films grown on such substrates grow with the [001] direction in the film plane and the [010] direction at 45° out of the film plane (for more details see section 3.1.1). Studies have shown that $SrRuO_3$ films grown on $SrTiO_3$ undergo two structural phase transitions - orthorhohmbic to tetragonal at $\sim 623°$ K and tetragonal to cubic at $\sim 873°$ K [87]. In our experiments, we use such films.

The strain in epitaxial growth further distorts the lattice structure of $SrRuO_3$. The substrate compress the lattice of the $SrRuO_3$ along [110] [001] and expand it along the [110] direction. This causes further tilting and rotating of the RuO_6 octahedra in thin films, relative to the bulk [86].

Transport and Thermodynamic Properties

The anomalous transport behavior of $SrRuO_3$ has attracted much interest. At room temperature, the resistivity of $SrRuO_3$ is of $\sim$200 $\mu\Omega cm$ and increases with temperature almost without saturation, and seems to cross the Iofe-Regel limit [88]. Terahertz conductivity and infrared conductivity show non-Drude [89, 90] behavior [91, 92]. Band calculations of $SrRuO_3$ at the paramagnetic phase show also an anisotropic behavior in Fermi velocities [93, 94, 95]. As temperature is lowered to its critical temperature ($\sim$ 150 K for thin films and $\sim$ 165 K for bulk material) a change in the resistivity is observed.

The behavior of the temperature derivative of the resistivity near T_c strongly deviates from Fisher-Langer theory [96, 97], and the resistivity shows negative deviations from Matthiessen's rule [98, 99, 100, 101]. Despite these anomalies, some of which strongly indicate non-fermi liquid (NFL) behavior, the resistivity at low temperature has $\rho = \rho_o + a\rho^2$ dependence [96, 97], the heat capacity obeys at low temperatures $C_v = \gamma T + \beta T^3$ [88], and quantum oscillations in the electrical resistivity at high magnetic fields (the Shubnikov-de Haas oscillations) show an existence of conventional fermion quasiparticles [102]. However, the coefficient, A, of the T^2 term in the resistivity is three orders of magnitude larger than elemental ferromagnets values. The measured linear heat capacity coefficient, γ, is 30 mJ/mol K^2, which is larger than one would estimate for typical metal and exceeds the theoretical value, calculated from band calculations, by a factor of 3.7. These high values of γ and A are evidence of strong electronic interactions. Since $SrRuO_3$ is a ferromagnetic material

magnetic effects have their influence on resistivity. These effects include a magnetoresistive behavior and AMR, OHE, EHE, PHE and Domain wall [103] contribution to resistivity [104, 105].

The EHE behavior of $SrRuO_3$, that depends on the normal component of magnetization [106, 107, 108, 109], is quite anomalous showing a sign change of the EHE coefficient at ∼127 K.

Although $SrRuO_3$ is almost cubic, it exhibits resistivity anisotropy. In our work we have determined the small resistivity anisotropy behavior above and below the critical temperature by using the PHE.

Magnetic Properties

$SrRuO_3$ is a ferromagnet with T_c ∼165 K for bulk materials and ∼150 K for films. Magnetism in $SrRuO_3$ is itinerant and it originates from the $4d$ electrons of the Ru atoms. The spontaneous magnetization in the zero-temperature limit in bulk (films) is 1.6 μ_B (1.4 μ_B), which is consistent with band calculations [93]. MCA studies of bulk single crystals have shown that there are two magnetic EA along the face diagonals of the pseudo-cubic unit cell, which are the orthorhombic [100] and [010] directions [110]. In contrast to bulk, epitaxial thin films of $SrRuO_3$ are characterized by a single EA whose orientation is temperature dependent [86, 111]. Above T_c, the EA coincides with [010], which is at 45° relative to the film normal, while below T_c there is a reorientation transition where the EA rotates in the (001) plane approaching 30° relative to the normal at 2 K [111]. The difference between the bulk and the thin films is probably a result of a further distortion of the already distorted bulk lattice by tilting and rotating the RuO6 octahedra. The MCA energy

can be described by $E = Ksin^2\theta$, with a weakly temperature-dependent anisotropy constant, $K \sim 1.2 \times 10^7$ erg/cm^3. The large MCA is mainly a result of crystal distortion and large spin-orbit coupling. By using the expression for the domain wall width $\pi(C/2K_1)^{1/2}$ [112, 113] where $K_1 \approx 10^7$ erg/cm^3 and $C = 2JS^2/a$ the width is estimated to be in the order of 3 nm. much smaller compared to other magnetic metals like nickel (∼72 nm), iron (∼30 nm) [114] and cobalt (∼15 nm).

2.2 NiFe alloys

Roughly speaking, magnetic materials for industrial purposes are divided into two categories: a) hard magnetic materials - materials that have high coercive field and b) soft magnetic materials that are easier to magnetize and have higher permeability. Between 1913 to 1921 Gustave Elman and his associates developed a new alloy containing nickel and iron elements with different relations (more information on the history of their investigation can be found in the book of Bozorth [115]). These alloys are commonly known as permalloys (Py). In most cases the name is followed by a number representing the percent of nickel in this alloy. In the range of 50 to 80 percent nickel, the alloy is all face centered cubic. For a nickel iron composition relation of 1:3 respectively, the alloy can undergo long range ordering below ∼776 K. The magnetization properties of the ordered alloy are inferior to those of the disordered alloy. In our work we used Py with 78 to 81 percent nickel.

Py 78, which we used in our work, has $T_c = 853^\circ$ K and a very high permeability. The permeability value depends on the sample treatment, giving, in some cases, initial permeability of 8000 and a maximum permeability of 100000. The coercive field of Py 78 gives, for some cases, 0.05 Oe with induction saturation (B_S) of 10800 Gauss [116]. Magnetization reversal experimental studies on Py layers of uniaxial magnetic anisotropy are found to fit theory [117].

The room temperature resistivity of Py 78 is 16 $\mu\Omega$-cm, and is significantly influenced by the magnetic field [118] with AMR of 3 to 4%. In permalloy 80 the scattering of spin down electrons can be 5 to 10 times higher than spin up electrons which implies mean free path $\lambda_\uparrow/\lambda_\downarrow = 5$ to 10 (typically $\lambda \uparrow = 6$ nm and $\lambda_\downarrow = 1$ nm

at 300 K) [119].

Permalloy has an important role in a variety of electrical components: a) loading coils, b) transformers, c) magnetic amplifiers, d) relays, e) flux gates and f) AMR sensors (for different applications including recording read head sensors).

Chapter 3

Experimental Details

3.1 Sample Fabrication

3.1.1 Fabrication of $SrRuO_3$ Films

In our research, we used high quality epitaxial thin films of $SrRuO_3$ grown on a $SrTiO_3$ substrate by Molecular beam epitaxy (MBE). In this method, the electron beam heats the Sr and Ru targets and causes their simultaneous evaporation on the substrate with the presence of atomic oxygen obtained by dissociating molecular oxygen using microwave plasma.

Figure 3.1: MBE system.

To create a sample with a single EA of magnetization it is necessary to break the cubic symmetry of the substrate surface. For this reason the substrate is miscut at an angle of 2^o. The miscut creates atomic steps with a height of 4 Åand a width of 114 Å. The $SrRuO_3$ film that grows on such a substrate grows with a uniform direction of magnetization [120, 121].

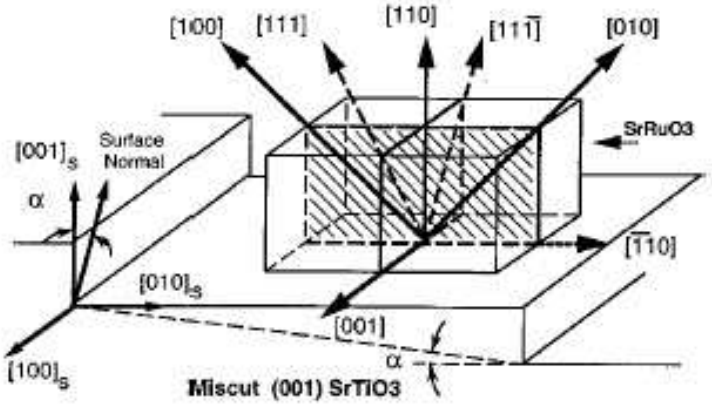

Figure 3.2: The lattice orientation of $SrRuO_3$ (110) films on miscut (001) $SrTiO_3$ substrate [86].

3.1.2 Fabrication of Ta/Py and Au Films

The magnetic permalloy films used in this work were fabricated to have no measured MCA. This was done by sputtering [122] monocrystaline substrates of SiO_2 with a polycrystaline film of Py (other works that study permalloy films indicate that sputtered Py has large magnetostriction only below 7 nm [123] while in our case we use Py layers of 10 nm). In this method, positive ions are accelerated towards a bulk target and sputter small particles off the target and onto the substrate. The sputtered Py layer is then protected by a capping layer of tantalum deposited by the

same technique. Further processing of the samples involved also sputtering of gold.

3.1.3 Plasma Reduction of Solutions

It was recently shown that plasma reduction of metallic ions from liquid solutions can be used as a coating method [124].

Plasma [125, 126, 127] is created when free electric charge is accelerated, one of the possibilities for this kind of procedure is by radio frequency (RF) oscillating electric field that is generated in the gas region. At sufficiently low pressures the combined effect of the electric field acceleration of electrons and elastic scattering of the electrons with neutral atoms or field lines leads to heating of the electrons. When electrons gain kinetic energy in excess of the first ionization threshold in the neutral gas species, electron - neutral collisions lead to further ionization, yielding additional free electrons that are heated in turn. Under electric field electrons oscillation frequency is given by:

$$\omega_p = \frac{4\pi n_e^2}{m_e} \tag{3.1}$$

Giving the relation between the charge density n_e and their frequency.

In this work we use plasma reduction in order to create metallic layers. In order to create these layers we used two kinds of plasma generators: a) The PDC-32G-2 plasma cleaner, and b) a microwave oven, modified to allow pumping and inserting gas into a vacuum chamber that was installed inside. The microwave higher frequency (2.45 GHz) and power (900 W) allowed us to reduce ions from solutions the first generater failed to reduce.

3.2 Patterning

For some of our patterns it was sufficient to use photolithography with a mask aligner. To fabricate samples with an approximate resolution of microns we used the SUSS MJB4 Manual Mask Aligner. This machine has the ability to print features with a resolution of 0.5 μm.

Figure 3.3: SUSS MJB4 Manual Mask Aligner for micron size resolution and HR-SEM Jeol JSM 7000F for sub micron patterning resolution.

For submicron patterns we used a "Raith" lithography system that was connected to a high resolution scanning electron microscope, HR-SEM (JSM-7000F). The Raith lithography system allowed us to pattern non patterned samples or to modify samples that are already patterned.

For monitoring the multipatterning process we used optical microscopes (Stereoscopic Zoom Microscope SMZ800 and "Material-Microscope Nikon L150") and HR-SEM.

In some of our work material analysis was performed. For these cases we used two systems: (a) bruker axs D8 advance powder x ray diffraction and (b) The energy dispersive X-ray spectroscopy (EDS) system which is connected to the HR-SEM and detects photons emitted from the sample surface due to electron collisions.

3.3 Measurement systems

To measure the magneto transport we used two systems: one that was designed to measure the transport at room temperature, and one that has the ability to measure several physical properties in a wide range of temperatures. Both machines are designed to enable 4 point measurement configuration [128, 129, 130, 131].

For room temperature measurements we used a homemade system which was designed and built as part of the research project.

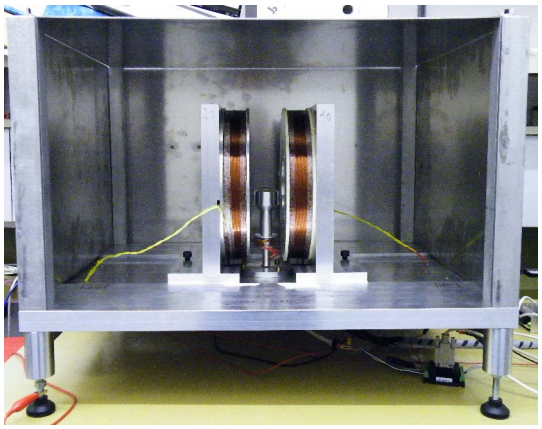

Figure 3.4: Room temperature measurement system.

The system is composed of two pseudo Helmholtz coils built of aluminum structure inside an isolated warped copper wire. The copper length for each coil is of 2500 meters. The interior radius is 38 mm and the exterior is 44.5 mm. The coils were designed to give a field change ($\Delta B/B$) of 3×10^{-7} Oe to a point located 5 mm aside (with the same distance from the two coils) for an external magnetic field of 372.6 Oe (compatible to a current of 1.8 A) field value sample laying between the coils. The sample itself is set on a stage that can rotate using a brushless motor (Faulhaber DC

24SR Micromotor) that is connected to a gear system. The stage can rotate more than 360° with an angle resolution of 0.03°. The sample is connected electrically to a switch box (Keithley 7001), a current source (Keithley 2400), and a nanovoltmeter (Keithley 2182). All measuring devices are computer controlled. The system itself is confined inside a metallic cage in order to reduce noise.

Low temperature measurements were preformed using a quantum design Physical properties measurement system (PPMS), with field range up to 9 T.

Chapter 4

Manuscripts

Determination of the resistivity anisotropy of $SrRuO_3$ by measuring the planar Hall effect

Isaschar Genish, Lior Klein, James W. Reiner, and M. R. Beasley;

Phys. Rev. B., 75, 125108, (2007).

Paramagnetic anisotropic magnetoresistance in thin films of $SrRuO_3$

Isaschar Genish, Yevgeny Kats, Lior Klein, James W. Reiner, and M. R. Beasley;

J. appl.; Phys., 95, 6681, (2004).

Local measurements of magnetization reversal in thin films of $SrRuO_3$

Isaschar Genish, Yevgeny. Kats, Lior Klein, James W. Reiner, and M. R. Beasley;

Phys. stat. sol. (C), 1 3440, (2004).

Plannar Hall effect sensors - effects of shape and size

Isaschar Genish, Yishai Sheperber, Gregory Saltira, Doron Aurbach , Lior Klein;

submitted.

Coating dielectric substrates by plasma-reduction of metallic ions in solvents[1]

Isaschar Genish, Alexander Irzh, Aharon Gedanken, Assaf Anderson, Arie Zaban, and Lior Klein;

submitted.

[1]Pended to patent

manuscripts

4.1 Determination of the resistivity anisotropy of $SrRuO_3$ by measuring the planar Hall effect

Determination of the resistivity anisotropy of $SrRuO_3$ by measuring the planar Hall effect

Determination of the resistivity anisotropy of $SrRuO_3$ by measuring the planar Hall effect

Determination of the resistivity anisotropy of $SrRuO_3$ by measuring the planar Hall effect

Determination of the resistivity anisotropy of $SrRuO_3$ by measuring the planar Hall effect

Determination of the resistivity anisotropy of $SrRuO_3$ by measuring the planar Hall effect

4.2 Paramagnetic anisotropic magnetoresistance in thin films of $SrRuO_3$

Paramagnetic anisotropic magnetoresistance in thin films of $SrRuO_3$

Paramagnetic anisotropic magnetoresistance in thin films of $SrRuO_3$

Paramagnetic anisotropic magnetoresistance in thin films of $SrRuO_3$

4.3 Local measurements of magnetization reversal in thin films of $SrRuO_3$

Local measurements of magnetization reversal in thin films of $SrRuO_3$

Local measurements of magnetization reversal in thin films of $SrRuO_3$

Local measurements of magnetization reversal in thin films of $SrRuO_3$

4.4 planar hall effect sensors - effects of shape and size

planar hall effect sensors - effects of shape and size

planar hall effect sensors - effects of shape and size

planar hall effect sensors - effects of shape and size

4.5 Coating dielectric substrates by plasma-reduction of metallic ions in solvents

Coating dielectric substrates by plasma-reduction of metallic ions in solvents

Coating dielectric substrates by plasma-reduction of metallic ions in solvents

Coating dielectric substrates by plasma-reduction of metallic ions in solvents

Coating dielectric substrates by plasma-reduction of metallic ions in solvents

Coating dielectric substrates by plasma-reduction of metallic ions in solvents

Coating dielectric substrates by plasma-reduction of metallic ions in solvents

Coating dielectric substrates by plasma-reduction of metallic ions in solvents

Coating dielectric substrates by plasma-reduction of metallic ions in solvents

Coating dielectric substrates by plasma-reduction of metallic ions in solvents

Coating dielectric substrates by plasma-reduction of metallic ions in solvents

Coating dielectric substrates by plasma-reduction of metallic ions in solvents

Coating dielectric substrates by plasma-reduction of metallic ions in solvents

Coating dielectric substrates by plasma-reduction of metallic ions in solvents

Coating dielectric substrates by plasma-reduction of metallic ions in solvents

Coating dielectric substrates by plasma-reduction of metallic ions in solvents

Coating dielectric substrates by plasma-reduction of metallic ions in solvents

Coating dielectric substrates by plasma-reduction of metallic ions in solvents

Bibliography

[1] B. D. Culity, Introudaction to Magnetic Materials, Addision-Wesley Publishing Company, 208, (1972).

[2] Sōshin Chikazumi, Stanley H. Charap, Physics of Magnetism, Robert E. Krieger Publishing Company, 114, (1978).

[3] K. Honda, S. Kaya, Sci. Reports Tohoku Univ, **15**, 721 (1926).

[4] N. S. Akulov, Zeits. F. Physik, **57**, 249; **59**, 254 (1929).

[5] R. M. Bozorth, Phys, Rev., **50**, 1076 (1936).

[6] J. D. Kleis, Zeits. Phys, Rev., **50**, 1178 (1936).

[7] J. H. Van Vleck, Phys. Rev., **52**, 1178 (1937).

[8] B. D. Culity, Introudaction to Magnetic Materials, Addision-Wesley Publishing Company, 50, (1972).

[9] B. D. Culity, Introudaction to Magnetic Materials, Addision-Wesley Publishing Company, **2**, 54, (1972).

[10] B. D. Culity, Introudaction to Magnetic Materials, Addision-Wesley Publishing Company, 242, (1972).

[11] E. M. Chudnovsky, L. Gunther, Phys. Rev. B., **37**, 9455, (1988).

[12] E. M. Chudnovsky, L. Gunther, Phys. Rev. Lett., **60**, 661, (1988).

[13] Pierre Weiss, J. de Physique, **6**, 661, (1907).

[14] B. D. Culity, Introudaction to Magnetic Materials, Addision-Wesley Publishing Company, 90, (1972).

[15] E. C. Stoner, E. P. Wohlfarth, Phil. Trans. Roy. Soc., **A-240**, 599, (1948).

[16] D. J. Craik, Structure and Proporties of Magnetic Materials, Pion Limited, 142, (1971).

[17] P K. H. J. Buscho, and F. R. de Boer, Physics of Magnetism and Magnetic Materials, Kluwer Academic Publishers, 63, (2003).

[18] K. H. J. Buschow, F. R. de Boer, Physics of Magnetism and Magnetic Materials, Kluwer Academic Publishers, 7, (2003).

[19] Friedel, J. (1969) in J. Ziman (Ed.) The Physics of Metals, Cambridge: Cambridge University Press, Vol. 1, p. 340.

[20] M. Kohler, Ann. Phys. (5), **32**, 211, (1938).

[21] J. M. Ziman, Electrons and Phonons, Oxford, 491, (1963).

[22] R. C. O'Handley, Modern Magnetic Materials, John Wiley and sons, 568, (2000).

[23] W. Thomson, Phil. Trans. Bakerian Lecture, (1856).

[24] W. Thomson, proc. Roy. Soc. of London, 8, 546, (1857).

[25] I.A. Campbell, Phys. Rev. Lett. **24**, 269, (1970).

[26] T. R. McGuire and R. I. Potter, IEEE Trans. Magn., **MAG-11**, 1018, (1975).

[27] P. Kapitza, Proc. Roy. Soc. A., **123**, 292, (1929).

[28] E. Justi, H. Scheffers, Metall-wirtschaft, **17**, 1359, (1938).

[29] J. Smit Physica 16, no. 6, (1951).

[30] Robert I. Potter, Phys. Rev. B., 10, 4626, (1974).

[31] W. Döring, Ann. Physik, **(**32) 259, (1938).

[32] E. Hall, Am. J. Math., **2**, 287, (1879).

[33] Neil W. Ashcroft, N. David Mermin, Solid State Physics, Saunders College Publishing, 11, (1976).

[34] J. Smit, Physica **21**, 877, (1955).

[35] J. Smit, Physica **24**, 39, (1958).

[36] L. Berger, Phys. Rev. B. **2**, 4559, (1970).

[37] M. V. Berry, Proc. R. Soc. Lond. A., **392**, 45, (1984).

[38] R. Karplus and J. M. Luttinger, Phys. Rev., **95**, 1154, (1954).

[39] J. M. Luttinger, Phys. Rev. **112**, 739, (1958).

[40] M.-C. Chang and Q. Niu, Phys. Rev. Lett., **75**, 1348, (1995).

[41] C. Goldberg and R. E. Davis, Phys. Rev., **94**, 1121, (1954).

[42] F. G. West, J. Appl. Phys. **34**, 1171 (1963).

[43] W. M. Bullis, Phys. Rev., **109**, 292, (1958).

[44] E. H. Putley, The Hall Effect And Semi-conductor Physics, Dover Publications, Inc., 25, (1968).

[45] G. A. Prinz, Science **282**, 1660, (1998).

[46] S. A. Wolf, D. D. Awschalom, R. A. Buhrman, J. M. Daughton, S. von Molnár, M. L. Roukes, A. Y. Chtchelkanova, and D. M. Treger, science **294**, 1488, (2001).

[47] I. *Žutić*, J. Fabian, and S. Das Sarma, Rev. Mod. Phys., **76**, 323, (2004).

[48] S. A. Wolf, A. Y. Chtchelkanova, and D. M. Treger, IBM J. Res. and Dev., **50**, 101, (2006).

[49] Albert Fert, Rev. Mod. Phys., **80 No. 4**, 1517, (2008).

[50] A. Fert, and I. A. Campbell, Phys. Rev. Lett., **21**, 1190, (1968).

[51] I.A. Campbell, A. Fert and O. Jaoul, J. Phys. C. (Metal Physics), **3**, S 95, (1970).

[52] A. Fert, and I. A. Campbell, J. Phys. (France), **32**, C1-46, (1971).

[53] A. Fert, and I. A. Campbell, J. Phys. F: Met. Phys., **6**, 849, (1976).

[54] P. M. Tedrow, R. Meservey, Phys. Rev. Lett., **26**, 192, (1971).

[55] M. Julliere, Phys. Lett., **54**, 225, (1975).

[56] Mark Johnson, R. H. Silsbee, Phys. Rev. Lett., **55**, 1790, (1985).

[57] M. N. Baibich, J. M. Broto, A. Fert, F. Nguyen Van Dau, F. Petroff, P. Eitenne, G. Creuzet, A. Friederich, and J. Chazelas, Phys. Rev. Lett., **61**, 2472, (1988).

[58] G. Binasch, P. Grünberg, F. Saurenbach, and W. Zinn, Phys. Rev. B., **39**, 4828, (1989).

[59] B. T. Jonker and M. E. Flatté, in Nanomagnetism, edited by D. L. Mills and J. A. C. Bland (Elsevier, New York), p. 227. (2006).

[60] S. Datta, and B. Das, Appl. Phys. Lett., **56**, 665, (1990).

[61] A. Cottet, T. Kontos, S. Sahoo, H. T. Man, W. Belzig, C. Bruder, and C. Schnenberger, Semicond. Sci. Technol., 21, 578, (2006).

[62] L. E. Hueso, J. M. Pruneda, V. Ferrari, G. Brunell, J. P. Valdes-Herrera, B. D. Simmons, P. B. Littlewood, E. Artacho, A. Fert, and N. D. Mathur, Nature (London) 445, 410, (2007).

[63] James E. Lenz, Procedings of The IEEE, **78**, 973, (1990).

[64] Direct-Current Magnetic Sensors for Soft Magnetic Materials, Preperd by Committee A-6 on Magnetic Properties, American Society for Testing and Materials (ASTM), Special Thecnical Publicaton, 371 S1, 25, (1970).

[65] Trifon M. Liakopoulos, Chong H. Ahn, Sensors and Actuators, **77**, 66, (1999).

[66] Evgeny B. Alexandrov, Viktor A. Bonch-Bruevich, Optical, Eng. **31 No. 4**, 711, (1992).

[67] M. Klank and O. Hagedorn, M. Shamonin, H. Dötsch, J. Appl. Phys., **92**, (2002).

[68] K. P. Koo and G. H. Sigel, Jr., Optics Lett., **7, No. 7**, (1982).

[69] A. Dandridge, A. B. Tveten, G. H. Sigel, E. J. West, and T. G. Giallorenzi, Electron. Lett., **16**, 408, (1980).

[70] G. D. Pitt, Technology of Chemicals and Materials for Electronics, Editor: E. A. Howells, Society of Chemical Industry, Ellis Horwood Limited, 261, (1984).

[71] Kamarinos, G. Viktorovitch, P. Cristoloveanu, S. Borel, J. Staderini, R., International Electron Devices Meeting, **23**, 114A, (1977).

[72] Radivoje S. Popović, and Rolf Widmer, IEEE Transactions on Electron Devices, **33, NO. 9**, 1334, (1986).

[73] D. Drung, R. Cantor, M. Peters, H. J. Scheer, and H. Koch, Appl. Phys. Lett., 406, **57 (4)**, (1990).

[74] J. Včelák, P. Ripka, J. Kubík, A. Platil, P. Kašpar, Sensors and Actuators A. 123, (2005).

[75] Derk Jan Adelerhof, Wim Geven, Sensors and Actuators **85**, 48, (2000).

[76] Hauser, H.: Magnetfeldsensor II. Austrian Pat. Appl. No. 1928/96, (1996).

[77] Hans Hauser, Johann Hochreiter, Gunther Stangl, Rupert Chabicovsky, Michael Janiba, Karl Riedling J. of Mag. Mat., 215-216, 788, (1996).

[78] Feng, J. S. Y., Romankiw, L. T. and Thompson, D. A.: Magnetic self-bias in the barber pole MR structure. IEEE Trans. Magn., **13**, 1466, (1977).

[79] A. Schoul, F. Nguyen Van Dau, J. R. Childress, Appl. Phys. Lett., **66 (20)**, 2751, (1995).

[80] F. Nguyen Van Dau, A. Schuhl, J.R. Childress and M. Sussiau. Transducers '95 eurosensors **9** 241, (1995).

[81] François Montigne, Alain Schoul, Frédéric Nguyen Van Dau, Armando Encinas, Sensors and Actuators, **81**, 324, (2000).

[82] F. N. Van Dau, A. Schuhl, J. R. Childress, M. Sussiau, Sensors and Actuators A., **53**, 256, (1996).

[83] Y. C. Chang, C. C. Chang, J. C.Wu, Z. H. Wei, M. F. Lai, and C. R. Chang, IEEE Transactions On Magnetics, **42, NO. 10**, 2963, (2006).

[84] John C. Slater, Quantum Theory of Molecules and Solids, **2** (Symmetry and Energy Bands In Crystals), McGraw-Hill Book Company, 68, (1965).

[85] C. B. Eom, R. J. Cava, R. M. Fleming, J. M. Fillips, R. B. vanDover, J. H. Marshal, J. W. P. Hsu, J. J. Krajewski, and W. F. Peck, Science, **258**, 1766, (1992).

[86] Q. Gan, R. A. Rao, C. B. Eom, L. Wu, and F. Tsui, J. Appl. Phys., **85**, 5297, (1999).

[87] J. P. Maria, H. L. McKinstry, and S. Trolier-McKinstry, Appl. Phys. Lett., **76**, 3382, (2000).

[88] P. B. Allen, H. Berger, O. Chauvet, L. Fano, T. Jarlborg, A. Junod, B. Revaz and G. Santi, Phys. Rev. B **53**, 4393, (1996).

[89] P. Drude, Annalen der physik **1**, 566 and **3** (1900).

[90] Neil W. Ashcroft, N. David Mermin, Solid State Physics, Saunders College Publishing, 2, (1976).

[91] P. Kostic, Y. Okada, N. C. Collins, Z. Schlesinger, J. R. Reiner, L. Klein, A. Kapitulnik, T. H. Geballe, and M. R. Beasley, Phys. Rev. Lett. **81**, 2498, (1998).

[92] J. S. Dodge, C. P. Weber, J. Corson, J. Orenstein, Z. Schlesinger, J. W. Reiner, and M. R. Beasley, Phys. Rev. Lett., **85**, 4932, (2000).

[93] P. B. Allen, H. Berger, O. Chauvet, L. Forro, T. Jarlborg, A. Junod, B. Revaz, and G. Santi, Phys. Rev. B **53**, 4393, (1996).

[94] D. J. Singh, J. Appl. Phys., **79**, 4818, (1996).

[95] G. Santi and T. Jarlborg, J. Phys.: Condens. Matter, **9**, 9563, (1997).

[96] L. Klein, J. S. Dodge, C. H. Ahn, G. J. Snyder, T. H. Geballe, M. R. Beasley, and A. Kapitulnik, Phys. Rev. Lett., **77**, 2774, (1996).

[97] L. Klein, J. S. Dodge, C. H. Ahn, J. W. Reiner, L. Mieville, T. H. Geballe, M. R. Beasley, and A. Kapitulnik, J. Phys.: Condens. Matter, **8**, 10111, (1996).

[98] Neil W. Ashcroft. N. David Mermin, Solid State Physics, Brooks/Cole, 323, (1976).

[99] J. M. Ziman, Electrone and Phonons, Oxford, 286, (1960).

[100] L. Klein, Y. Kats, N. Wiser, M. Konczykowski, J. W. Reiner, T. H. Geballe. M. R. Beasley and A. Kapitulnik., Europhys. Lett., textbf55(4), 532, (2001).

[101] Y. Kats, and L. Klein, Phisica B., **793**, 312, (2002).

[102] A. P. Mackenzie, J. W. Reiner, A. W. Tyler, L. M. Galvin, S. R. Julian, M. R. Beasley, T. H. Geballe, and A. Kapitulnik, Phys. Rev. B., **58**, R13318, (1998).

[103] H. N. V. Temperley, Changes of State, Cleaver-Hume Press Ltd, 209, (1956).

[104] L. Klein, Y. Kats, A. F. Marshall, J. W. Reiner, T. H. Geballe, M. R. Beasley, and A. Kapitulnik, Phys. Rev. Lett., **84**, 6090, (2000).

[105] M. Feigenson, L. Klein, J. W. Reiner, and M. R. Beasley, Phys. Rev. B., **67**, 134436. (2003).

[106] M. Izumi, K. Nakazawa, Y. Bando, Y. Yoneda and H. Terauchi, J. Phys. Soc. Jpn., **66**, 3893, (1997).

[107] L. Klein, J. R. Reiner, T. H. Geballe, M. R. Beasley, and A. Kapitulnik, Phys. Rev. B., **61**, R7842, (2000).

[108] Z. Fang, N. Nagaosa, K. S. Takahashi, A. Asamitsu, R. Mathieu, T. Ogasawara, H. Yamada, M. Kawasaki, Y. Tokura, and K. Terakura, Science, **302**, 92, (2003).

[109] R. Mathieu, C. U. Jung, H. Yamada, A. Asamitsu, M. Kawasaki, and Y. Tokura, Phys. Rev. B., **72**, 064436, (2006).

[110] G. Cao, S. McCall, M. Shepard, J. E. Crow, and R. P. Guertin, Phys. Rev. B., **56**, 321, (1997).

[111] L. Klein, J. S. Dodge, C. H. Ahn, J. W. Reiner, L. Mieville, T. H. Geballe, M. R. Beasley and A. Kapitulnik, J. Phys.: Condens. Matter, **8**, 10111, (1996).

[112] B. D. Culity, Introudaction to Magnetic Materials, Addision-Wesley Publishing Company, 290, (1972).

[113] Sōshin Chikazumi, Stanley H. Charap, Physics of Magnetism, Robert E. Krieger Publishing Company, 188, (1978).

[114] B. D. Culity, Introudaction to Magnetic Materials, Addision-Wesley Publishing Company, 291, (1972).

[115] bozorth, Richard M., Ferromagnetism, 968, (New York) Van Nos, (1951).

[116] B. D. Culity, Introudaction to Magnetic Materials, Addision-Wesley Publishing Company, 529, (1972).

[117] D. O. Smith, J. Appl. Phys., **29**, 264, (1958).

[118] T. T. Chen, V. A. Marsocci, solid state comm, **10**, 783, (1972).

[119] Edited by Etienne du Tremolet de Lacheisserie, Damien Gignoux, Michel Schlenker, Magnetism, **2** (Materials and Applications), Springer, 282, (2005).

[120] L. Klein, J.S. Dodge, C.H. Ahn, J.W. Reiner, L. Mieville, T.H. Gaballe, M.R. Beasley and A. Kapitulnik, J.Phys. Condens. Matter, **8**, 10111, (1996).

[121] A. F. Marshall, L. Klein, J. S. Dodge, C. H. Ahn, J. W. Reiner, L. Mieville, L. Antognazza, A. Kapitulnik, T. H. Geballe, and M. R. Beasley, J. Appl. Phys., **85**, 4131, (1999).

[122] R. A. Coombe, The Electrical Proporties and Applications of Thin Films, Sir Isaac Pitman and Sons Ltd., 4, (1967).

[123] Y. K. Kim, T. J. Silva, Appl. Phys. Lett., **68 (20)**, (1996).

[124] Ji-Jun Zou, Yue-ping Zhang, and Chang-Jun Liu. Langmuir, **22 (26)**, 11388, (2006).

[125] E. M. Lifshitz and L. P. Pitaevskii, Physical Kinetics, Landau and Lifshitz Course of Theoretical Physics Volume 10, Pergamon Press, 129, (1981).

[126] H. Conrads and M. Schmidt Plasma Sources Sci. Technol. **9**, 441, (2000).

[127] F. F. Chen, Intrudaction to Plasma, Plenum Press, 73, (1974).

[128] M. Büttiker, Phys. Rev. Lett., **57**, 1761, (1986).

[129] M. Büttiker, IBM J. Res. and Dev. **50**, 101 (2006).

[130] L. J. van der Pauw, Philips Research Reports, **13**, 1, (1958).

[131] L. J. van der Pauw,Philips Technical Review, **20**, 220, (1958).